U.I.T.

UNIONE ITALIANA DI TERMOFLUIDODINAMICA

ATTI
XIX CONGRESSO NAZIONALE SULLA TRASMISSIONE DEL CALORE

19th UIT National Heat Transfer Conference

ESTRATTO

A cura di:

Editor: Paolo Tartarini
Facoltà di Ingegneria - Sede di Modena
Università di Modena e Reggio Emilia

Modena, 25 - 27 Giugno 2001

UNIVERSITÀ DI MODENA E REGGIO EMILIA
Facoltà di Ingegneria - Sede di Modena

IN-TUBE EVAPORATION OF R134a AND R22 INSIDE A NEW MICROFIN TUBE

Adriano Muzzio, Alfonso Niro

Dipartimento di Energetica, Politecnico di Milano, I-20133 Milano, Italy

ABSTRACT

This paper presents experimental data on heat transfer coefficients and pressure drops in saturated flow boiling of oil-free R22 and R134a inside a 9.52-mm microfin tube of new design and, for comparison, in a smooth tube with the same outside diameter. Both the tubes are horizontally operated. The microfin tube is characterized by 82 sharp fins alternating with two different heights, that is the distinguishing feature from other new microfin tubes. The effect of mass flux, average quality and overall quality change on heat transfer characteristics have been separately investigated. Data here reported are for a nominal temperature of 5 °C with mass flux ranging from 90 to 440 kg/ s m^2, inlet quality from 0.1 to 0.65 and quality change between 0.1 and 0.7. For the microfin tube, refrigerant R22 exhibits higher heat transfer coefficients and lower pressure gradients than R134a; indeed, the enhancement factor comes up to 3.8 for R22 but to 2.9 for R134a whereas the penalty factor varies with *G* within the range of 1.25-1.0 for R22 and of 1.0-1.35 for R134a. Consequently, the tested microfin tube may be used with some convenience for the evaporation of R134a only at low mass fluxes.

1. INTRODUCTION

The need for high performance compact heat exchange equipment has led to the development of many types of surfaces that enhance heat transfer coefficient. In air-conditioners and refrigerators, the reduction of the air-side thermal resistance to that of the refrigerant side has urged industry to focus on in-tube augmentation of evaporation/condensation heat transfer. Among the enhancement techniques developed, e.g. rough surfaces, twisted-tape insert and low-finning, one of the most promising is the microfin tube since the pressure drop penalty caused is generally less than the associated heat transfer increase, as shown in many experimental studies. This is not generally the case of other enhancement techniques as reported by Schlager et al. [1] in their survey on in-tube augmentation.

The micro-fin tube, which is characterized by numerous small fins that spiral down the inside surface of the tube, was first reported in the open literature in the mid 1970's; in the subsequent years an increasing number of additional papers reporting on boiling and condensation of refrigerants inside these tubes were published. Its historical development, modification and performance are described by Schlager [2] and Webb [3]. The majority of these studies are for R12, R113 and R22 especially, both in boiling and condensation for the latter. For evaporation, a survey of the relevant literature shows that with the aforementioned refrigerants the heat transfer enhancement factor, defined as the ratio of the heat transfer coefficient of a microfin tube to that of a comparable smooth tube, ranges between 1.6 and 3.3. For condensation, typical values of the heat transfer enhancement factor vary from 1.6 to 2.9. In both cases, pressure drop increases are described as slight or very little.

More recently, the phase-out of CFC and HCFC refrigerants imposed by the problem of ozone layer depletion and the tightening of the energy-efficiency standards to reduce global warming due to the greenhouse effect, have caused a redirection of research towards testing pure and blended alternative refrigerants and the development of microfin tubes of advanced design. However, flow boiling of R134a in microfin tubes has not been thoroughly investigated.

Eckels an Pate [4] studied evaporation and condensation of HFC-134a and CFC-12 in a smooth tube and in a microfin tube at various test conditions. For R134a, heat transfer enhancement factor varied from 1.5 to 2.5 during evaporation and from 1.8 to 2.5 during condensation. For both the refrigerants, the pressure drop penalty factor, defined as the ratio of pressure drop in the microfin tube to that in a comparable smooth tube, was less than the corresponding enhancement factor. However, in the case of R134a at the lowest temperature and highest mass flux, the penalty factor slightly exceeded the enhancement factor. Torikoshi et al. [5,6] measured the mean evaporation and condensation heat transfer coefficients and pressure drops for R134a in a plain tube and in a micro-fin tube. In evaporation, the latter augmented the heat transfer by a factor of 2 compared to the smooth tube. With mixtures of refrigerant and oil, they also noted that the micro-fin tube was more influenced by the presence of oil. Singh et al. [7] reported local flow boiling heat transfer coefficients of R134a in a micro-fin tube as a function of parametric values of mass flux, quality and heat flux in the electrically heated test section. Oh and Bergles [8] examined in-tube evaporative heat transfer of R-134a in a smooth tube and five micro-fin tubes. Spiral angles of 6, 12, 18, 25 and 44 degrees were tested at constant mean diameter and number of fins. The optimal spiral angle was found to be mainly dependent on the mass flux.

This paper presents data on saturated flow-boiling of R134a

in a smooth tube and a micro-fin tube of new design, developed by Trefimetaux, which is characterized by a double series of alternating fins of different heights. The paper also reports comparisons with data, previously obtained by the authors [9], on flow-boiling of R22 in the same microfin tube.

2. EXPERIMENTS

2.1 Experimental Apparatus

A schematic diagram of the experimental facility is shown in Figure 1. The rig is composed of three independent circuits, namely, a refrigerant circuit, a heating/cooling water circuit and a chilled coolant (water-glycol solution) circuit.

The refrigerant circuit mainly consists of a boiler, the test section, a condenser, a gear pump and a filter dryer. Liquid and vapor are drawn from the boiler through two distinct lines. A subcooler and a mass flow-meter are mounted on the liquid line whereas a superheater and two float-type flow-meters are installed on the other line. Subcooler and superheather ensure a single-phase flow through the flow-meters for any operating conditions. The liquid and vapor flow rates are controlled by precision metering valves. Downstream of the valves, vapor and liquid streams are mixed; the resulting two-phase mixture flows through a 1.5 m long calming section and then it enters the test tube, that is the inner tube of a double-pipe heat exchanger. At the exit, the refrigerant is discharged into a shell-and-coil condenser; a gear pump conveys the refrigerant from the condenser to the boiler.

The heating/cooling circuit supplies the water flowing in the annulus outside the test tube. This circuit is composed by a centrifugal pump, a plate heat exchanger and a bath vessel equipped with a 5-kW heater controlling the water temperature. A magnetic flow-meter is used to measure the water flow rate through the test section annulus. Finally, the chilled coolant circuit is filled with a water-glycol solution and it supplies the cold medium circulating into heat exchangers mounted on the refrigerant and water circuits. A commercial refrigeration unit is used as chiller.

The test section is divided into two identical subsections mounted in series; each subsection is 1.3-m long with an effective heat transfer length of 1.12 m, that is the distance between the inlet and outlet ducts of the outside tube. At the inlet of test section, a temperature probe is mounted inside the tube countercurrently to the refrigerant flow. Such a probe consists of a 0.25-mm, K-type thermocouple plugged into a L-shaped, 8-cm long, 2-mm o.d. tube that is located at the centerline of the duct. In addition, at the entrance and exit of the first subsection and at the outlet of the second one, there are two pressure-taps. Downstream the exit pressure taps of each subsection there is a sight glass made of 85-mm long, 8.5-mm i.d., pyrex smooth tube; sight glasses are neither heated or cooled. Finally, each subsection is equipped with four T-type thermocouples to measure wall temperatures; the thermocouples are placed in pairs on the top and the bottom of the test tube. Each thermocouple is cemented in a longitudinal groove cut in the outside wall of the test tube, with the tip at 140 mm from the tube end and at 50 mm from the inlet/outlet duct of the outside annulus. Calming and test sections are thermally insulated by a 10-cm thick, glass-wool covering that ensures a measured thermal resistance of 4 K/W.

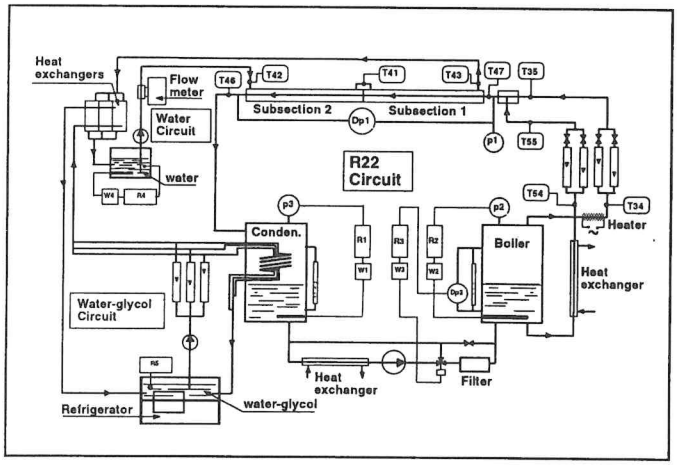

Figure 1. Schematic diagram of the experimental facility.

2.2 Test Procedures and Data Reduction

Signals from thermocouples and transducers are cyclically read by a data acquisition unit and sent to an on-line PC. In order for all variables to be affected by similar RMS relative errors, the measurements of refrigerant temperature, pressure drop and water flow rate are based on 30, 50 and 100 readings for cycle, respectively. Every experimental value, instead, is obtained by averaging the measurements of ten cycles in order to reduce the influence of random errors and fluctuations. Finally, for every operative condition, more than ten experimental data are collected.

The heat transfer coefficient is computed as follows. We assume the refrigerant temperature varies linearly between the value T_{in}, measured at the entrance of the test section, and the value T_{out} computed at the exit as $T_S(p_S(T_{in}) - \Delta p)$, where T_S is the function correlating the saturation temperature to the pressure, p_S the inverse function of T_S, and Δp the pressure drop measured along the test section. Then, for each subsection we calculate the mean refrigerant temperature $T_{r.m,i}$, the mean wall temperature $T_{w.m,i}$, the refrigerant to wall temperature mean difference $\Delta T_{m,i}=(T_{w.m,i}-T_{r.m,i})$, and the heat transfer coefficient $h_i=q_i/\Delta T_{m,i}$ where q_i is the mean heat flux based on a nominal inside area corresponding to the maximum internal diameter, i.e., the diameter at the root of microfins. Eventually, we compute the average heat transfer coefficient for the test section as the arithmetic mean of the subsection coefficients h_i. Relevant variables for the present investigation are affected by the following representative experimental uncertainties measured or estimated by an error propagation analysis: ±2.8% for the refrigerant mass flow rate, ±1.3% for the inlet quality, ±0.2 K between the refrigerant temperature and the saturation one, ±1.0% for the refrigerant pressure drop, ±1.0% for the water volume flow rate, ±0.02 K for the water temperature difference between the subsection inlet and outlet, ±1.4% for the heat rate, and ±7% for the average heat transfer coefficient.

3. RESULTS AND DISCUSSION

In saturated flow boiling, for a fixed section configuration (shape, dimensions and orientation with respect to gravity), average heat transfer coefficient and pressure drop depend on four independent variables, namely, total mass flow rate, temperature (or pressure), inlet thermodynamic quality and

Figure 2. Drawing of the microfin cross-section profile.

TUBE Parameter		HVA	Smooth
Outside diameter	[mm]	9.52	9.52
Maximum inside diameter	[mm]	8.62	8.92
Bottom wall thickness	[mm]	0.45	0.30
Higher fin height	[mm]	0.20	-
Lower fin height	[mm]	0.17	-
Apex angle		40°	-
Number of grooves		82	-
Helix angle		18°	-
Heat transfer internal surface ratio		1.84	1
Actual cross-section surface ratio		0.946	1

Table 1. Geometrical parameters of the tested tubes.

heat rate or quality change over the section, being the fluid everywhere saturated.

The experimental data here reported were obtained with refrigerants R134a and R22 inside a 9.52-mm microfin tube of new design developed and manufactured by Trefimetaux, i.e., Metofin 952-45HVA 40/82. Data for both refrigerants on a smooth tube with the same outside diameter are also reported for comparison. The microfin tube is characterized by numerous sharp fins, i.e., an apex angle of 40 degrees, alternating with two different heights as shown in Figure 2. The latter is the distinguishing feature from other new microfin tubes. Table 1 lists geometrical parameters of the microfin and smooth tubes, as well as the heat transfer internal surface ratio and the actual cross-section ratio with respect to the smooth tube.

Tests were carried out at a nominal saturation temperature of 5 °C (±0.2 K) corresponding to a pressure of 0.35 and 0.58 MPa for R134a and R22, respectively. Total mass flow rate, inlet thermodynamic quality and quality change were varied in turn while keeping the others constant in order to demonstrate clearly the effect of each variable against the others. The total mass flow rate ranged from 5.56 to 25 g/s corresponding to a mass flux G, with respect to a nominal cross-section area based on the maximum internal diameter, that varies between about 90 and 440 kg/s m^2. The inlet quality x_{in} was varied from 0.1 to 0.65 whereas the quality change Δx from 0.1 to 0.7.

In Figure 3, the average heat transfer coefficient h_b is plotted versus the mass flux G for the microfin and smooth tubes; data are obtained at an inlet quality x_{in}=0.3 and a quality change Δx=0.3. In considering this figure, it is worth to note that mass flux variations at constant Δx imply proportional variations in heat flux because of their linear dependence; for the data reported in figure, the average heat flux ranges from 5.2 to 24 kW/m^2. As expected, the heat transfer coefficient is an increasing function of G with higher values for the HVA-tube. Regarding the working fluid, the coefficients for R22 inside the HVA-tube are greater than those for R134a while the smooth tube shows nearly the same values for both the refrigerants. Differences in thermal performances are well accounted by the enhancement factor. A plot of this factor versus G is shown in Figure 4. As seen, the enhancement factor comes up to 3.8 for R22 but to 2.9 for R134a; in both cases, it is a decreasing function of the mass flux and asymptotically tends to about 1.4, that is a value smaller than the internal surface ratio. This result disagrees with the conclusion by Eckels and Pate [10] that at high mass flux the heat transfer augmentation is due to the area increase only, whereas geometry seems to affect fluid dynamics and heat transfer even at high G, as observed by Ito and Kimura [11], too. Finally, the performance differences between R134a and R22 inside the HVA-tube are also due to a joint effect of geometry and thermodynamic properties, as they vanish for the smooth tube.

Figures 5 and 6 show the dependence of h_b on the average quality x_m for a quality change Δx=0.3 at mass fluxes G=238 and 143 kg/s m^2, respectively (G=222 and 133 kg/s m^2 for the smooth tube). For G=238 kg/s m^2, the microfin tube exhibits values continuously increasing with x_m in the tested quality

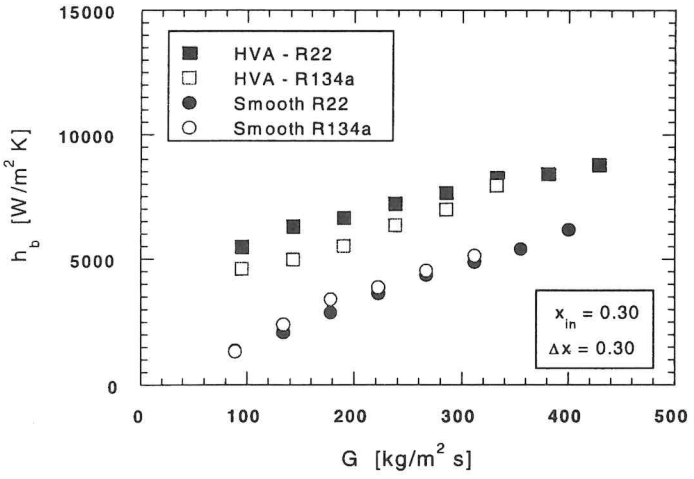

Figure 3. Heat transfer coefficient h_b versus mass flux G for fixed inlet quality x_{in} and quality change Δx.

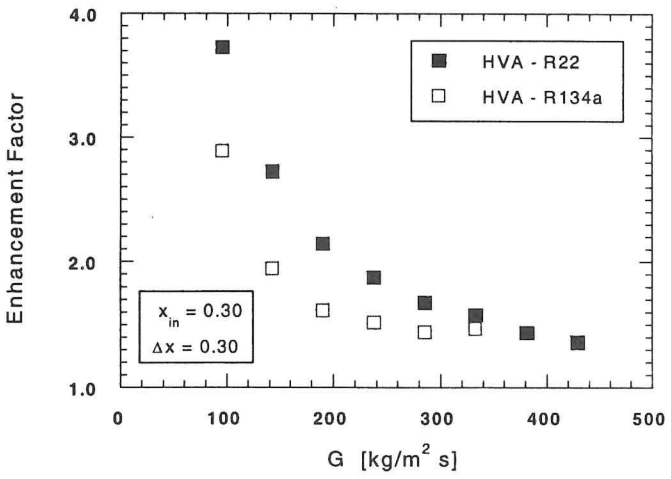

Figure 4. Enhancement Factor versus mass flux G for fixed inlet quality x_{in} and quality change Δx.

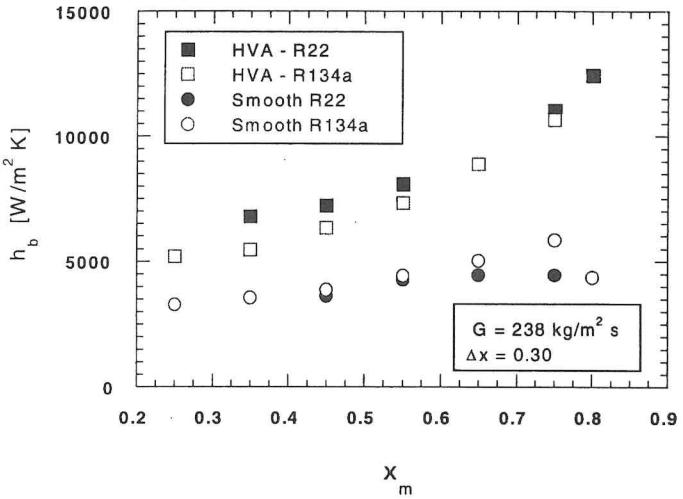

Figure 5. Heat transfer coefficient h_b versus average quality x_m for fixed mass flux G=238 kg/m^2 s and quality change Δx.

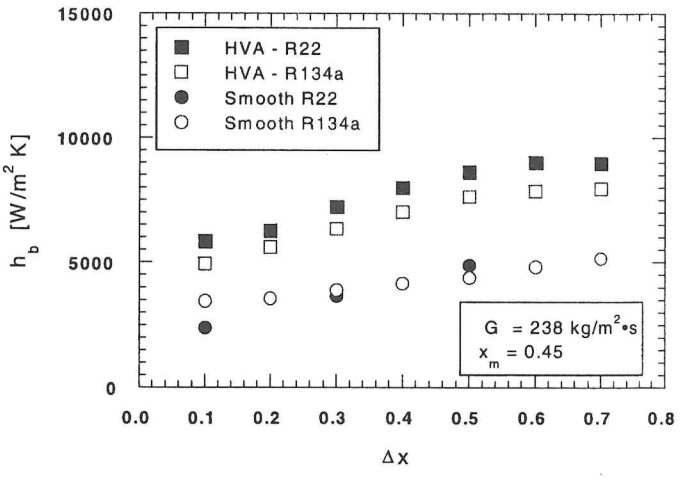

Figure 7. Heat transfer coefficient h_b versus quality change Δx for fixed mass flux G and average quality x_m.

range, while the data for the smooth tube are characterized by a maximum although slightly marked (it is worth warning that the value at x_m=0.8 for R134a inside the smooth tube is affected by a larger uncertainty because heat transfer process in the second subsection was strongly unsteady). As the decrease is due to the deterioration of heat transfer in postdryout region, these data seem to suggest that microfins shift the dryout occurrence toward higher values of quality. However, this conclusion is not confirmed at the lower value of G, since the data reported in Figure 6 display a maximum at x_m=0.75 for both the tubes. It is interesting to remark the peculiar trend of data for the HVA-tube: the heat transfer coefficient weakly depends on x_m for values smaller than 0.55, while it becomes an increasing function of x_m from 0.55 to 0.75; a further increase in x_m, eventually, results in a fall off of h_b. Supported by visual observations, we conjecture that in the first region the flow is stratified and, therefore, the heat transfer is dominated by nucleate boiling that is quite insensitive to quality. As transition to annular flow occurred, convective boiling mechanism becomes dominant in the heat transfer process and h_b increases with x_m up to the dryout occurrence. When x_m is further increased, the dryout onset moves upstream and the postdryout region spreads out; since this region is characterized by a considerably lower heat transfer, the average heat transfer coefficient quickly decreases with x_m. This effect is clearly highlighted by the data, not reported here, for each subsection; indeed, the heat transfer coefficient for the first subsection is a strictly increasing function of x_m while that for the second one displays a maximum at x_m =0.9.

Finally, the influence of Δx and, therefore, of the heat flux on the heat transfer coefficient is shown in Figure 7 for values of G=238 kg/s m^2 and x_m=0.45. As seen, h_b is an increasing function of Δx for both tubes up to approximately Δx=0.7, while at higher values the curve for the HVA-tube flattens and eventually reverses because of the dryout occurrence. Also in this case, the microfin tube exhibits heat transfer coefficients for R22 greater than R134a, while the corresponding values for the smooth tube are nearly the same for both the refrigerants although the data for R134a display a weaker growth rate. Finally, if we compare the Figures 6 and 7, it is interesting to observe that in the latter the dryout already occurs for an outlet quality of about 0.8, while the data reported in Figure 6, taken at the same mass flux, do not exhibit a maximum even at x_m=0.75 corresponding to an

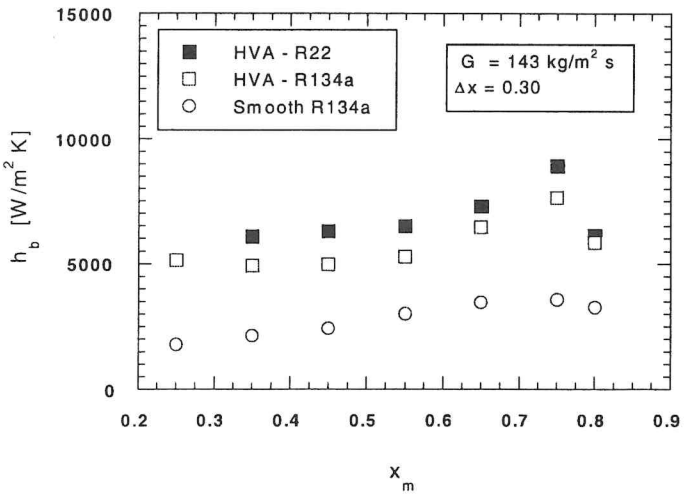

Figure 6. Heat transfer coefficient h_b versus average quality x_m for fixed mass flux G=143 kg/m^2 s and quality change Δx.

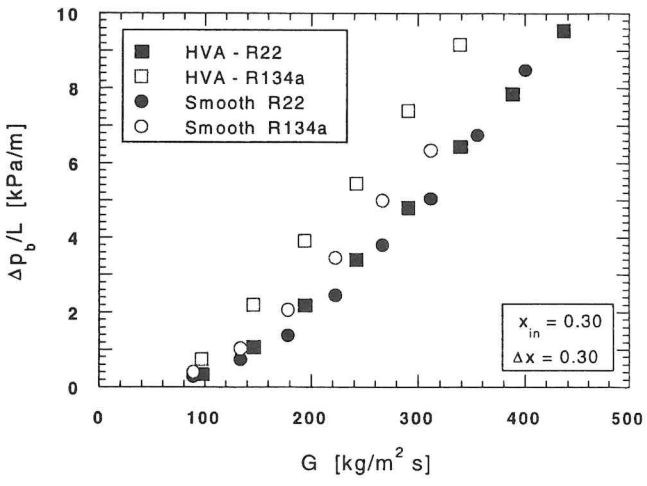

Figure 8. Pressure drop per unit length versus mass flux G for fixed inlet quality x_{in} and quality change Δx.

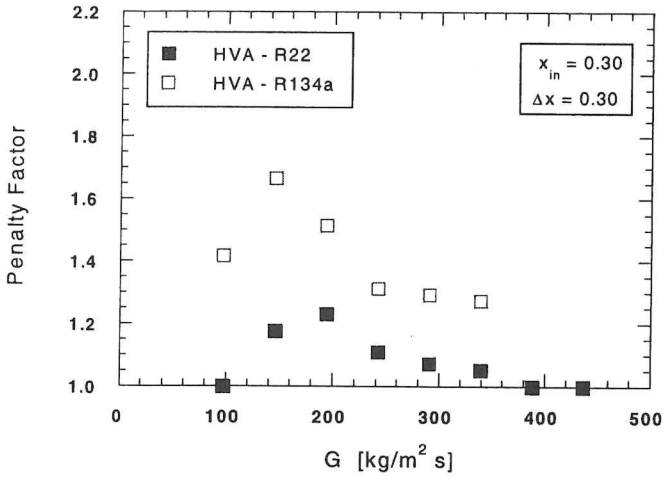

Figure 9. Pressure drop penalty factor versus mass flux G for fixed inlet quality x_{in} and quality change Δx.

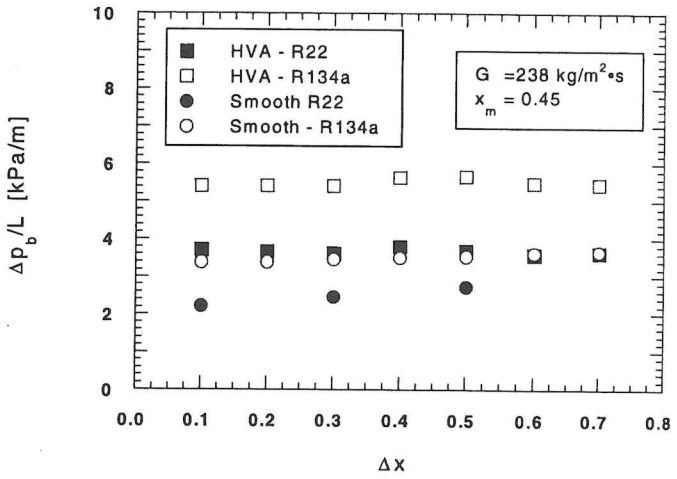

Figure 11. Pressure drop per unit length versus quality change Δx for fixed mass flux G and average quality x_m.

outlet quality of 0.95. We conjecture this effect is caused by the different values of heat flux that amounts to about 33 kW/m^2 for the data reported in Figure 7, whereas it is about 17 kW/m^2 for the others.

Figure 8 shows the data of pressure drop per unit length $\Delta p_b/L$ plotted versus the mass flux G obtained for the same conditions reported in Figure 3, i.e., x_{in}=0.3 and Δx=0.3. As seen, pressure gradients for R134a are considerably higher than those for R22 and, moreover, the increase in $\Delta p_b/L$ between the microfin and smooth tubes is more pronounced for R134a. This result is clearly displayed in Figure 9 where the Penalty Factor is plotted versus G; the values for R134a range between 1.35 and 1.8, resulting from 25% to 50% higher than those for R22 which come up to 1.25 at the most. Finally, for both the tubes the ratio (Δp_{R134a} / Δp_{R22}) is a decreasing function of G which seemingly tends to one.

The effects of average quality x_m and quality change Δx on pressure gradients are shown in Figures 10 and 11, respectively, for the same conditions of Figures 5 and 7. As observed, pressure gradients are quite sensitive to variations of x_m but almost independent on Δx; moreover, the pressure gradient does not exhibit a monotonic increasing dependance on quality at a constant mass flux, but it increases up to a maximum and then it decreases toward the value for pure vapor flow

Finally, Figure 12 shows the efficiency index, i.e., the ratio of Enhancement Factor to Penalty Factor, is plotted versus the mass flux at the same conditions for the data reported in Figures 4 and 9, namely, x_{in}=0.3 and Δx=0.3. For R134a, this index is everywhere nearly equal to one except for G=97 kg/m^2 s where it is 1.9, whereas for R22 the it varies between 3.7 and 1.4. This result suggests that the HVA-tube may be used with R134a with some convenience only at low mass fluxes.

4. CONCLUSIONS

1. The heat transfer coefficients for R22 inside the HVA-tube are higher than those for R134a while the smooth tube shows nearly the same values for both the refrigerants. The enhancement factor, which turns out to be a decreasing function of the mass flux, comes up to 3.8 for R22 but to 2.9 for R134a at the lower values of G and it asymptotically tends to 1.4 in both cases. The latter value

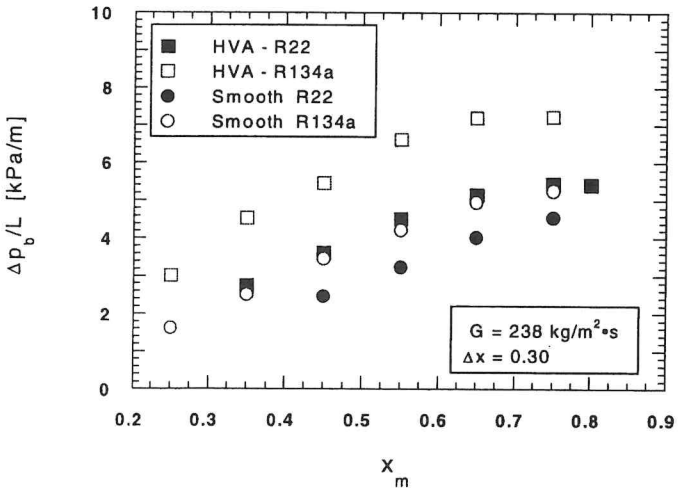

Figure 10. Pressure drop per unit length versus average quality x_m for fixed mass flux G and quality change Δx.

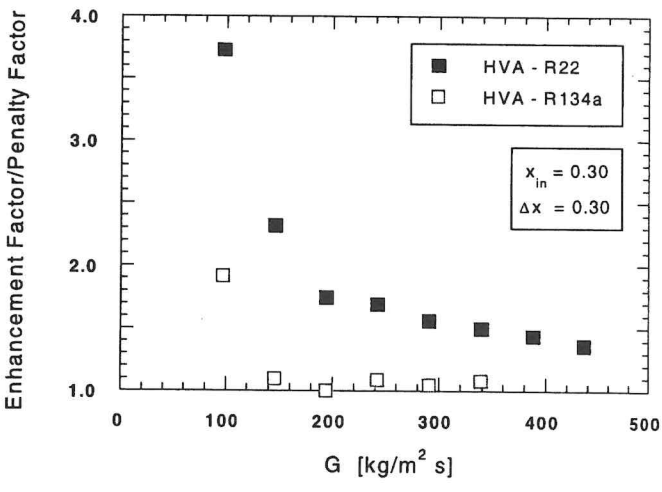

Figure 12. Efficiency Index versus mass flux G for fixed inlet quality x_{in} and quality change Δx.

is smaller than the internal surface ratio.

2. For both the refrigerants, data on heat transfer coefficient as a function of quality seem to suggest that micro-finning shifts dryout occurrence toward higher values of quality. However, this effect is dependent upon mass flux, being more pronounced at higher values of G.
3. For both smooth and microfin tubes, refrigerant R134a exhibits higher pressure gradients than R22, when comparison is made at the same values of saturation pressure, mass flux, average quality and mean heat flux. What is more, the increase in pressure gradient between the microfin tube and the smooth tube is more pronounced for R134. Consequently, the penalty factors for R134a are higher than those for R22 and vary with G within the range of 1.8-1.35 and 1.25-1.0, respectively.
4. The efficiency index varies with G, at constant average quality and mean heat flux, from 3.7 to 1.4 for R22 whereas for R134a it flattens around 1.0 except at G=97 kg/m^2 s where it comes up to 1.9. This result suggests that the HVA-tube may be used with R134a with some convenience only at low mass fluxes.

5. ACKNOWLEDGEMENTS

This work is supported by MURST (the Italian Department for the University and for the Scientific and Technical Research) via PRIN 1999 grants.

6. REFERENCES

1. Schlager, L.M., Bergles, A.E, Pate, M.B, "A survey of refrigerant heat transfer and pressure drop emphasizing oil effects and in-tube augmentation", *ASHRAE Transactions*, Vol. 93, Part. 1, pp. 392-416, 1987.
2. Schlager, L.M., "Boiling and Condensation in Microfin Tubes", in "Industrial Heat Exchangers", Lecture Series 1991-04, von Karman Institute for Fluid Dynamics, Rhode Saint Genèse, Belgium, 1991.
3. Webb, R.L., "Principles of Enhanced Heat Transfer", John Wiley & Sons, Inc., New York, 1994.
4. Eckels, S.J., Pate, M.B., "Evaporation and Condensation of HFC-134a and CFC-12 in a Smooth Tube and a Micro-fin Tube", *ASHRAE Transactions*, Vol. 97, Part. 2, pp. 71-81, 1991.
5. Torikoshi, K., Kawabata, K., Ebisu, T., "Heat transfer and pressure drop characteristics of HFC-134a in a horizontal heat transfer tube", Proceedings of the 1992 International Refrigeration Conference, Purdue University, pp. 167-176, 1992.
6. Torikoshi, K., Kawabata, K, Ebisu, T., "In-tube heat transfer and pressure drop characteristics of R-134a, R-32 and mixture of R-32/R-134a inside a horizontal tube", *ASHRAE Transactions*, Vol. 99, 1993.
7. Singh, A., Ohadi, M.M., Dessiatoun, S., "Flow Boiling Heat Transfer Coefficients of R-134a in a Microfin Tube", *J. Heat Transfer*, Vol. 118, pp. 497-499, 1996.
8. Oh, S., Bergles, A.E., " Experimental Study of the Effects of the Spiral Angle on Evaporative Heat Transfer Enhancement in Microfin Tubes", *ASHRAE Transactions*, Vol. 104, Part. 2, pp. 1137-1143, 1998.
9. Muzzio, A., Niro, A., "Evaporation and condensation of R22 inside two microfin tubes of new design", Proccedings of the 3rd European Thermal Sciences Conference, Vol. 2, pp. 957-962, Heidelberg, September 10-13, 2000.
10. Eckels S.J., Pate, M.B., "Evaporation heat transfer coefficients for R-22 in micro-fin tubes of different configurations", HTD-Vol. 202, pp. 117-125, 1992.
11. Ito, M., Kimura, H., "Boiling Heat Transfer and Pressure Drop in Internal Spiral-Grooved Tubes", *Bulletin of JSME*, Vol. 2, No. 171, pp. 1251-1257, 1979.